Structural Engineering and Mechanics, *Vol. 69, No. 6 (2019) 591-605*
DOI: https://doi.org/10.12989/sem.2019.69.6.591

Evaluation of performance and seismic parameters of eccentrically braced frames equipped with dual vertical links

Vahid Mohsenian[a] and Ali Nikkhoo*

Department of Civil Engineering, University of Science and Culture, Tehran, Iran

(Received June 14, 2018, Revised January 20, 2019, Accepted January 28, 2019)

Abstract. Investigations on seismic performance of eccentrically braced frames equipped with dual vertical links have received little attention. Therefore, the main goal of this paper is to describe design steps for such frames and evaluate nonlinear performance of this system according to the reliability analysis. In this study, four and eight story frame structures are analyzed and the response modification factors for different intensity and damage levels are derived in a matrix form based on a new approach. According to the obtained results, the system has high ductility and acceptable seismic performance. Moreover, it is concluded that using response modification factor equal to 8 in the design of system provides desirable seismic reliability under the design and maximum probable hazard levels. Due to desirable performance and significant advantages of the dual vertical links, this system can be used as a main lateral load bearing system, in addition to its application for rehabilitation of damaged structures.

Keywords: eccentric bracing; dual vertical link; demand response modification factor; capacity response modification factor; reliability analysis; fragility curves

1. Introduction

The eccentric braced system can provide both required stiffness and strength because of existence of the yielding fuse and the bracing members. The lateral seismic performance of this system is combination of the flexural-shearing behavior of fuses and the compressive-tensile performance of the braces. Different configurations for the seismic fuse are possible. It can be placed in story elevation as a distinct section of the beam or located vertically and connected to the beam. The second configuration has the following advantages:

1. Yielding and rotation of the link surely has no effect on the story beam and diaphragm. In fact, when the vertical links are used, damages due to lateral loading occur far from the beam and story level.
2. The vertical links after severe earthquake can be replaced easily. While, in the case of horizontal links, the link and story beam are integrated, thus cannot be replaced after earthquake. Therefore, it is obvious that using the vertical link would considerably reduce maintenance and rehabilitation cost of a structure.

Because of its simple mechanism, possible replacement and ease of design and construction, this system is not only applicable for the new structures, but also to strengthen and rehabilitate the existing and damaged structures. This system was introduced by Seki *et al*. (1988) as a new lateral load bearing system. Their studies showed that the hysteresis curves of the new system is very stable and symmetric. In another study, Baradaran *et al.* (2015) evaluated performance of the eccentric braced frames equipped with vertical links and found out that such structures have desirable behavior and high energy dissipation capacity.

Daryan *et al*. (2008) study the effect of the steel type (mild and hard) on performance of the vertical links. This study demonstrated that utilizing mild steel for the construction of the fuse would considerably improve performance of the frame structure by increasing its energy dissipation capacity.

Massah and Dorvar (2014) investigated the performance of the steel braced frames equipped with the vertical links made of shape memory alloys (SMA). Their findings proved that using the SMA would improve ductility, stiffness and lateral strength and moreover the reversibility. This study indicated that using the links made of SMA would result in reduction of both inter-story drift and the permanent drift.

Experimental and analytical studies of Sabouri-Ghomi and Saadati (2014) revealed that performance and deformations of the vertical links can be predicted easily by means of numerical analysis. In their study, the results of the experimental and analytical analysis for the location of damage initiation and deformation modes were the same. Furthermore, they presented that increase in length of the vertical link, reduces its critical load, rotation capacity and stiffness. Accordingly, they suggested the appropriate length for the beam is the one to cause shear yielding.

Shayanfar *et al.* (2008) investigated seismic performance of the braced steel frames equipped with the

*Corresponding author, Associate Professor
E-mail: nikkhoo@usc.ac.ir
[a]M.Sc. Student

http://www.techno-press.com/journals/sem&subpage=7
ISSN: 1225-4568 (Print), 1598-6217 (Online)

dual vertical links. They observed that during yielding of the links, no instability occurs. Moreover, they reported stable and wide hysteresis curves for dual vertical links. Based on their obtained results, they proposed this system for design of the new earthquake resistant building as well as for rehabilitation of existing structures.

According to the experimental and analytical studies of Lian and Su (2017), using high strength steel for the beams and columns in the eccentric braced frames equipped with vertical links results in improvement in the hysteresis behavior, energy dissipation and lateral load bearing capacity.

Based on the studies of Rahnavard *et al.* (2017), application of dual links in the eccentric bracing system, in addition to improving hysteresis behavior, increases capacity of the frame considerably. This study displayed that increasing distance between the vertical links results in better performance of the frame structure.

Experimental studies of Duan and Su (2017) on the eccentric braced with vertical links made of high strength steel showed that load bearing capacity of shear deformable specimen is higher than the flexural one.

In the performed experimental and analytical analysis (Vetr *et al.* 2017, Bouwkamp *et al.* 2016), design relations are proposed for the design of eccentric frame structures which are equipped with vertical links. According to these studies, the ultimate shear strength is reported to be about 2.2 times the nominal strength and P-Delta effects are negligible.

Based on the investigations performed by Zahrai and Parsa (2015), when the vertical link has sufficient support, even with reduction of the width of its wing, the hysteresis curves will be stable.

Based on studies of Zahrai and MoslehiTabar (2013) on frame structures with shear links, increasing length of the vertical link would increase the probability of brittle fracture due to multi-axial stresses.

Shayanfar *et al.* (2011) investigated the effects of the stiffeners for the web of vertical links on performance of structure. According to their findings, stiffeners improve ductility by postponing shear buckling of the web. They proposed details for design of composite vertical links. Based on their suggestions, concrete prevents premature buckling of the link web.

In the experimental studies of Zahrai and Mahroozadeh (2010), rotation angle of the link beam before failure is reported between 0.128 to 0.156 radian. Moreover, the average equivalent damping between 26.7 to 30.6 percent and response modification factors about 7.15 to 10.65 results in acceptable ductility of the frames. They stated that in their study, almost all of the applied energy to the structures are dissipated by the vertical links and the assumption of elastic performance of beams, columns and braces is completely valid.

In most of the performed studies about eccentric braced structures equipped with vertical links, the single links are used. A thorough literature review demonstrated that the previous investigations about application of dual vertical links are very limited and so far no study has been performed in order to determine the response modification factor for this system, especially in multi-story structures. Therefore, in this study, seismic performance and response modification factor for eccentric braced frames with dual vertical links for different levels of earthquake intensities and acceptable damages in the frame and links are evaluated by means of a new approach based on nonlinear behavior and reliability analysis, and reported in the matrix form. The new presented approach for determination of the response modification factor, in addition to evaluation of reliability of the proposed response modification factors in the available standards and design codes, provide design flexibility for the designers. In other words, the designer is able to select a response modification factor in accordance to a specific hazard level and the probable damage based on that intensity.

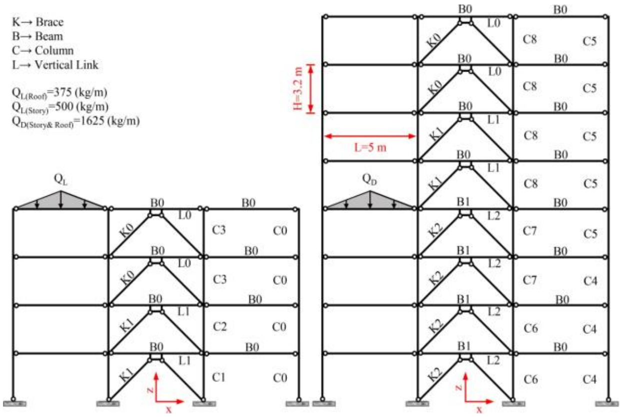

Fig. 1 Geometrical properties and gravitational loading of the modeled frame structures

Table 1 Specifications of the structural members

Symbol	Section	Symbol	Section	Symbol	Section
C0	2IPE12	C6	BOX(40×40×2.5)	B0	IPE24
C1	BOX(30×30×2.0)	C7	BOX(35×35×1.5)	B1	IPE30
C2	BOX(25×25×1.0)	C8	BOX(30×30×0.8)	L0	IPE8
C3	BOX(25×25×0.5)	K0	2UNP10	L1	IPE10
C4	2IPE16	K1	2UNP12	L2	IPE12
C5	2IPE14	K2	2UNP14	*	*

Dimensions are reported in “cm”

2. Methodology

2.1 Properties of the modeled frame structures

In this study, 4 and 8 storey structures as shown in Fig. 1 are used. Both buildings are residential and designed for the area with very high seismic hazard (design ground acceleration equals to 0.35 g). The storey height and span length are taken equal to 3.2 and 5 m, respectively. According to the classification provided by the Iranian Seismic Code of Practice (Standard No. 2800), the site soil is type “II” which is equivalent to type “C” as prescribed by ASCE/SEI 41-13 (2014) 375(m/s)$\leq V_s \leq$750(*m/s*).

It should be noted that in Fig. 1, Q_D and Q_L represent story dead and live loads, correspondingly. As it could be seen, based on the roof type and loading area of the frame in plan, these loads are uniformly distributed over the story beams.

The studied frame structures are designed based on the Iranian National Building Code for steel structures design Part 10 (2008) and by employing ETABS software (CSI 2015). The equivalent static approach is used for preliminary design of structures. By using response modification factor equal to 7 for the frames (according to the suggested value by the Iran's 2800 code for the special eccentric braced frame), the base shear coefficient is computed to be 0.125 for the structures.

It must be stated that in the braced spans, all of the force-control parameters in the braces, story beams and columns which have brittle and inductile failure, are controlled for the intensified earthquake (Ω_0=2).

Effect of the rigid story diaphragm and coupling of the story nodes are included in the developed models. Properties of the structural members (including beams, columns, braces and vertical links) are presented in Table 1. The modulus of elasticity and Poisson's ratio of steel (St_{37}) are taken equal to 210 GPa and 0.3, respectively.

Moreover, according to Fig. 1, the frames are symmetric with respect to the "*z*" axis.

2.2 Modeling nonlinear behavior and parameter evaluation

In order to model and analyze the structures in the range of nonlinear behavior, PERFORM-3D (CSI 2016) is used. As it is evident in Fig. 1, columns connections at the base level and beam to column connection in the side spans are hinged. It is obvious that the nonlinear behavior is not expected for these elements. Accordingly, these structural members (columns and beams of the side spans) are modeled by standard sections with the assumption of linear behavior.

In order to control failure mechanisms, evaluation of the interaction of structural elements in the braced spans and estimation of extent of the energy dissipation in these elements, in addition to the vertical links, story beams (in the braced span) and braces are also modeled as nonlinear elements. In the following sub-sections, the modeling process of each group of elements is described in details.

2.2.1 Modeling of brace elements

According to ASCE41-13 (2014), for the braces with hinge connections, in which energy absorption occurs due to formation of axial hinges, the axial deformation at the expected buckling load (Δc) and tensile load corresponding to the yield strength (Δt) are selected as ductility criteria and nonlinear behavior, respectively.

According to the connection of these elements, axial deformation of the brace is computed by using Eq. (1), in which, *L* is the free length of the brace

$$\Delta = FL / EA \tag{1}$$

It is evident that by replacing *F* with expected strength of the brace in tension (T_{CE}) and the lower bound of the strength under compression (P_{CL}), the two parameters (Δt) and (Δc) would be computed, correspondingly.

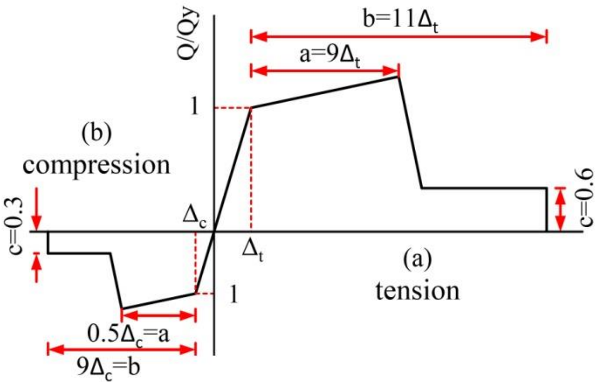

Fig. 2 Load-deformation multi-linear curve for steel components

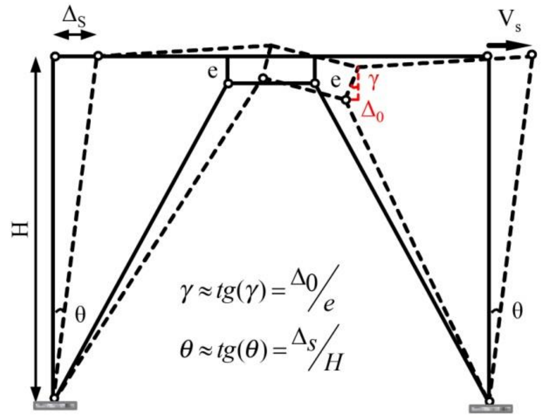

Fig. 3 Deformation of the frame elements under lateral loading (Schematic)

It should be noted that *A* and *E* in Eq. (1) are cross section area and modulus of elasticity, respectively.

In this study, modeling and control of the acceptance criteria for the braces in the nonlinear range of behavior is performed based on the generalized load-deformation curve which is depicted in Fig. 2.

Parameters a, b and c are extracted from the table of acceptance criteria for steel components in accordance with the yield type and section properties of the brace (double channel in this study) (ASCE/SEI 41-13 2014).

According to Fig. 3, the analysis of the eccentric braced frame equipped with dual vertical link reveals that after shear yielding of the vertical links, the axial force (*F*) and therefore tensile and compressive deformations in the bracings remain constant. Consequently, in high earthquake intensities, the only results of increase in the story drift (Δs) would lead to an increase in the shear strains of the vertical link. Obviously, it is necessary to consider this fact during design of the bracing members.

It is worthwhile stating that if the story beam is strong enough and thus, the failure of the links occurs at the first stages of loading, deformations in the story beam would be removed and this element retains its horizontal position.

The braces are modeled using the "Steel bar/Tie/Strut" element which only sustains axial loading.

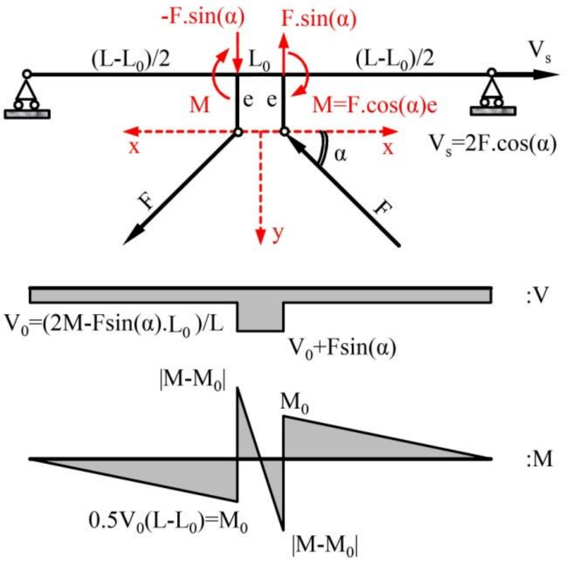

"V_s"→The story shear

"L"→The length of story beam

Fig. 4 Free-body diagram of the story beam and variation of shear force and bending moment

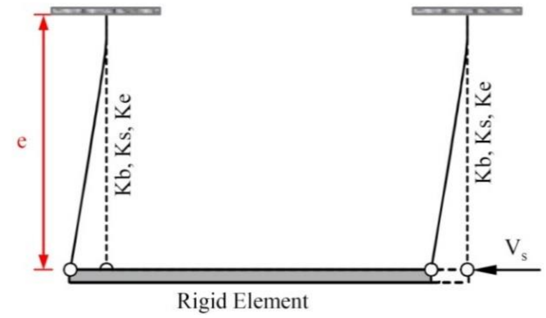

Fig. 5 Deformation of the link beams (Schematic)

2.2.2 Modeling of beams in the braced spans

Based on the free diagram of the story beam which is depicted in figure 4 and by using equilibrium equations, it is concluded that shear force is constant along the beam. In the location of the link connection to the beam, a step is evident in the shear diagram. The story beam experiences higher shear force in the area between to links. Moreover, the maximum bending moment also occurs in the location of link connection to the beam due to the concentrated bending moment, *M*. The shear and bending moment diagrams illustrate that increasing distance between vertical links (L_0) results in reduction of the maximum shear and moment in the beam story.

In this assembly, a little lower than the story level, there is another horizontal element at the end of the links where the braces are connected.

In the present study, length of this element (centerline to centerline of two vertical links) is taken equal to 30 cm. It must be noted that this element is design such that it is rigid in comparison with the vertical links. Therefore, the lateral stiffness of the story can be computed easily by using Eqs. (2) to (4) and according to the Fig. 5. It is possible to incorporate the mentioned horizontal elements in the absorption of applied energy to the structures due to severe earthquakes by appropriate selection and design of the sections and connection properties. Nevertheless, this process and determination of the optimum length for the horizontal element can be investigated in the future research works.

Based the previous explanations, the linear "beam" elements with concentrated "bending-rotational type" and "shear-plastic strain type" hinged at the critical locations are used in the software to model beams. It is noteworthy that the expected bending and shear capacities are derived by $Z.F_{ye}$ and $0.55F_{ye}A_w$, respectively. In these relations, A_w and Z are plastic modulus and web area of the beam (without consideration of the flange thickness) correspondingly and F_{ye} is the expected yield stress of steel.

Stiffness of each vertical link, k_e, is computed by using Eq. (2), as a function of shear (k_s) and bending stiffness (k_b), as well as support conditions. (Fig. 5).

$$k_e = \frac{k_s.k_b}{k_s + k_b} \tag{2}$$

$$k_s = \frac{G.A_w}{e} \tag{3}$$

$$k_b = \frac{3E.I_b}{e^3} \tag{4}$$

In these relations, I_b, E and G are section modulus, modulus of elasticity and shear modulus of the fuse material, respectively. Due to symmetry and parallel performance of the links, it is obvious that story stiffness is two times of each vertical link stiffness.

2.2.3 Modeling vertical links

The vertical links are designed such that they experience yielding before the other structural elements and therefore, they perform as seismic fuse under the design earthquake.

To achieve desirable behavior and shear yielding of the vertical links, length of these elements "e" are taken equal to 20 cm (Bathaei and Zahrai 2017). After computation of the expected bending and shear capacity using equations $Z.F_{ye}$ and $0.55F_{ye}A_w$, the selected length of the elements (e=20 cm) is compared with the ratio of $1.6M_{CE}/V_{CE}$.

Evaluations indicate that the vertical links surely experience shear yielding ($e \leq 1.6M_{CE}/V_{CE}$). Thus, in definition of curve of the link nonlinear behavior, the expected shear strength (V_{CE}) will be used. After designing the link sections based on the mentioned description, capacity and rotation angle of the elements (γ) is computed by consideration of the real loading conditions of the frame (interaction of shear force and bending moment) using ABAQUS (2014). The derived curve is idealized as an equivalent bilinear curve for use in the PERFORM-3D. It should be noted that the shear capacity of the sections is in good agreement with the results obtained via the equation $0.55F_{ye}A_w$. Shear deformation angle of the link (γ) is another important design parameter. In the present study, the shear deformation angle of vertical links in the intensified

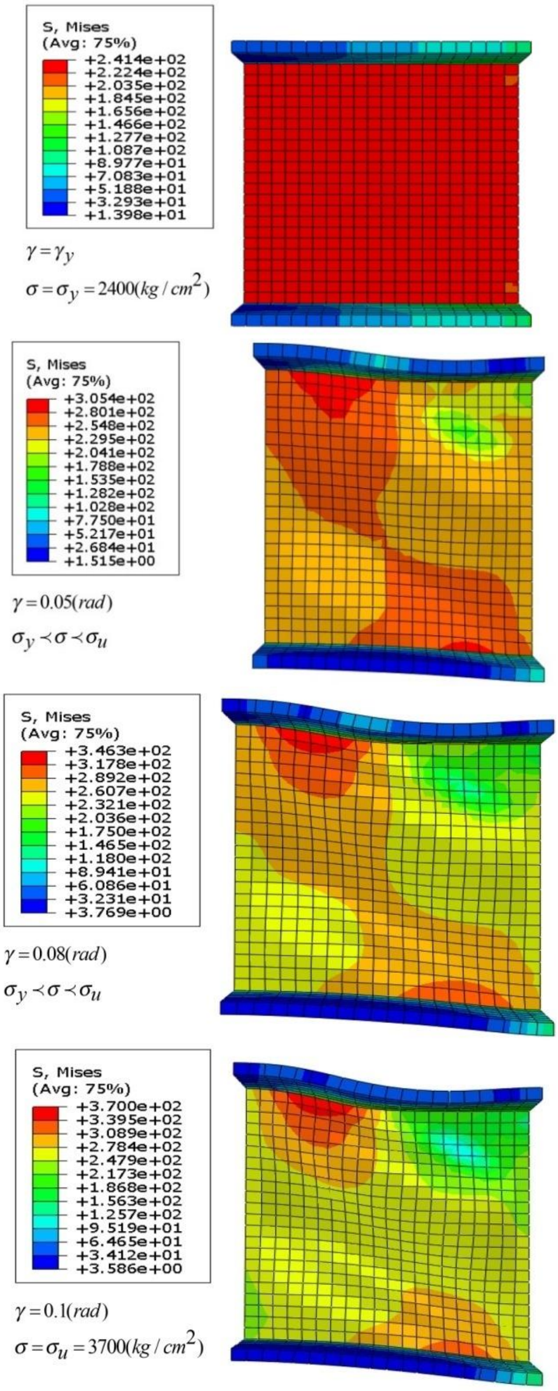

Fig. 6 Example of the deformations and maximum stresses in the links

earthquake is limited. In addition to calculation and modification of the capacity-deformation curves of the links, four different damage states are considered for the links, according to Fig. 6. As it is evident in this figure, the stresses in the wings are always less than web of the links. This observation verifies accuracy of the developed nonlinear model and the assumption of shear yielding in the link.

The linear "column" elements with concentrated "shear hinges-plastic strain type" are used for modeling the vertical links.

Table 2 Vibration periods (T) and effective translational mass coefficient (M) of the models for the first four modes of vibration

Mode No.	4 Story frame		8 Story frame	
	T(sec)	M (%)	T(sec)	M (%)
1	0.2135	84.52	0.3868	75.3
2	0.0795	12.44	0.1431	17.18
3	0.0476	2.06	0.079	3.98
4	0.0345	0.99	0.0544	1.64

3. Frame analysis

Assumption of the gravitational loading for both linear and nonlinear analyses are the same. It should be noted that the upper limit of the gravitational loads according to Eq. (5), is used for combination of lateral and vertical loads (ASCE41-13 2014).

$$Q_G = 1.1\left[Q_D + 0.2Q_L\right] \tag{5}$$

Where, Q_D and Q_L are dead and live loads, respectively.

3.1 Eigen value analysis

In the present section, the vibration periods and the effective translational mass participation factor of the frames for the first four modes of vibration are calculated. The obtained results are listed in Table 2.

Utilizing the empirical relations proposed by Iran's seismic design code provisions (Eq. (6)), the vibration periods of the 4 and 8 story frames are derived equal to 0.54 and 0.91sec, respectively. Eq. (7) which is suggested for the conventional concentric bracing system, gives the vibration periods of the frames equal to 0.34 and 0.57, correspondingly.

$$T = 0.08(H)^{0.75} \tag{6}$$

$$T = 0.05(H)^{0.75} \tag{7}$$

In these relations, H is the height of structures from base level in meter.

The vibration periods of the models show that the elastic stiffness of the system is higher than moment frames and the conventional concentric and eccentric braced frames. Moreover, the proposed empirical relations by the seismic code seem inappropriate for these systems, due to considerable difference between analytical and empirical values of the vibration periods. This is more evident via Eq. (6). Based on these observations, the system provides remarkable stiffness. Hence, in many of the rehabilitation projects, the vertical links could be used for improving stiffness of the damaged frame structures.

Trend of variation in the coefficients of effective translational mass for different modes demonstrates that increase in the height would increase participation of higher modes. Values of the vibration period (less than 1 s) and the effective translational mass participation factors (more than 75 percent) for the first mode show that the assumption of triangular distribution of the earthquake forces along the height of structure is acceptable.

3.2 Pushover analysis

The aim of this section is the evaluation of failure mechanisms of the system and determination of damage levels in deformations corresponding with the proposed design hazard level of the code. In the pushover analysis, the pattern of the lateral load must be identical as much as possible with what happens in earthquakes.

In the present study, the modal load pattern for lateral loading is used. In this pattern, the effective modes that account for 90 percent of the mass participation are combined together (Table 2). It is noteworthy that the target roof displacement is derived from the time history analysis and by taking average of the results obtained from artificial accelerograms (Table 3).

When there is good agreement between site conditions and properties of the selected ground motions, it is obvious that the resulted artificial accelerograms would be appropriate. Having the demand spectrum of the site, it is easy to produce artificial accelerograms close to the demand spectrum by means of wavelet conversion (Hancock *et al.* 2006). In this study, 12 artificial accelerograms are produced by modification of the existing accelerograms with the wavelet conversion based on the demand spectrum of the site according to the Iranian Seismic Code of Practice (Standard No. 2800) for the soil type “II” (equivalent to type “C” as classified byASCE/SEI 41-13 2014) and the first hazard level (return period equal to 475 year) (Standard No. 2800 2014). These accelerograms are applied to the structure (Fig. 7). The maximum acceleration of these accelerograms, which are called demand earthquake, is close to the design earthquake (0.35 g). It is noteworthy to say that the twelve earthquakes in Table 4 are used for production of artificial acelerograms.

In the following, in addition to evaluation of the damage stages of the modeled frame structures in the pushover analysis, drift of the roof (ratio of the roof displacement to the total height of structure) when the first yielding occurs at the beam and links of the braced frame is recorded. For this purpose, in the computer model, each time a series of the nonlinear elements are considered. It is evident that separation point of these curves is the desired response. Moreover, the roof drifts for the cases, in which, vertical links reach limit states depicted in Fig. 6 (when the shear strains of the links reach to 0.05, 0.08 and 0.1 radian for the first time) are also recorded. These values are depicted in Fig. 8.

The results of the pushover analysis proved that the first yielding occurs in the vertical links. In addition, it is observed that rate of the shear strain variation in both links are the same. For comparison, lateral stiffness of the four story frame is 1.7 times of that of the eight story structure. There is no sudden drop of strength and stiffness due to buckling of the braces in capacity curve of the frames. This observation proves that the vertical links act as seismic fuse and the force level of the braces remain constant after yielding of the braces.

In the following, according to the Fig. 9, at the target displacement, various parameters including axial force of braces, shear and moment of the story beam and shear strain of the vertical links are recorded.

Once more, the obtained results demonstrate acceptable

Table 3 The maximum drift corresponding with the design hazard level of the code (%)

8 story frame	4 story frame
0.1602	0.1135

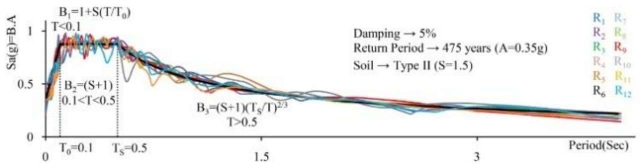

Fig. 7 Comparison of artificial spectra (R_i) with site demand spectrum

Table 4 The selected accelerograms which are consistent with the site condition in order to produce artificial accelerograms and doing incremental dynamic analysis

Record Number	Earthquake& Year	Station	R[1](km)	Component	M_W[2]	PGA(g)
R1	Cape Mendocino, 1992	Eureka – Myrtle & West	41.97	90	7.1	0.1782
R2	Northridge, 1994	Hollywood – Willoughby Ave	23.07	180	6.7	0.2455
R3	Northridge, 1994	Lake Hughes #4B - Camp Mend	31.69	90	6.7	0.0629
R4	Cape Mendocino, 1992	Fortuna – Fortuna Blvd	19.95	0	7.1	0.1161
R5	Northridge, 1994	Big Tujunga, Angeles Nat F	19.74	352	6.7	0.2451
R6	Landers, 1992	Barstow	34.86	90	7.4	0.1352
R7	San Fernando, 1971	Pasadena – CIT Athenaeum	25.47	90	6.6	0.1103
R8	Hector Mine, 1999	Hector	11.66	90	7.1	0.3368
R9	Kobe, 1995	Nishi-Akashi	8.70	0	6.9	0.5093
R10	Kocaeli (Turkey), 1999	Arcelik	53.7	0	7.5	0.2188
R11	Chi Chi (Taiwan), 1999	TCU045	77.5	90	7.6	0.5120
R12	Friuli (Italy), 1976	Tolmezzo	15.82	0	6.5	0.4169

[1] Closest Distance to Fault Rupture
[2] Moment Magnitude

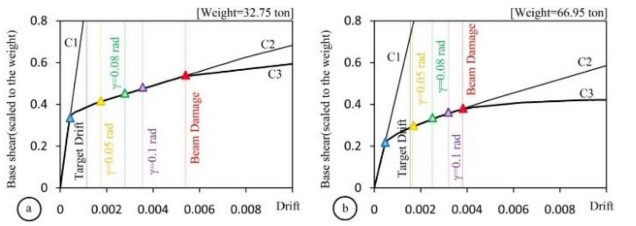

C1→ Elastic model
C2→ Inelastic model (only beams are elastic)
C3→ Inelastic model

Fig. 8 Capacity curves of the studied frame structures and drift values corresponding with damage limit states of the vertical links and the story beams (a)-4 story frame (b)-8 story frame

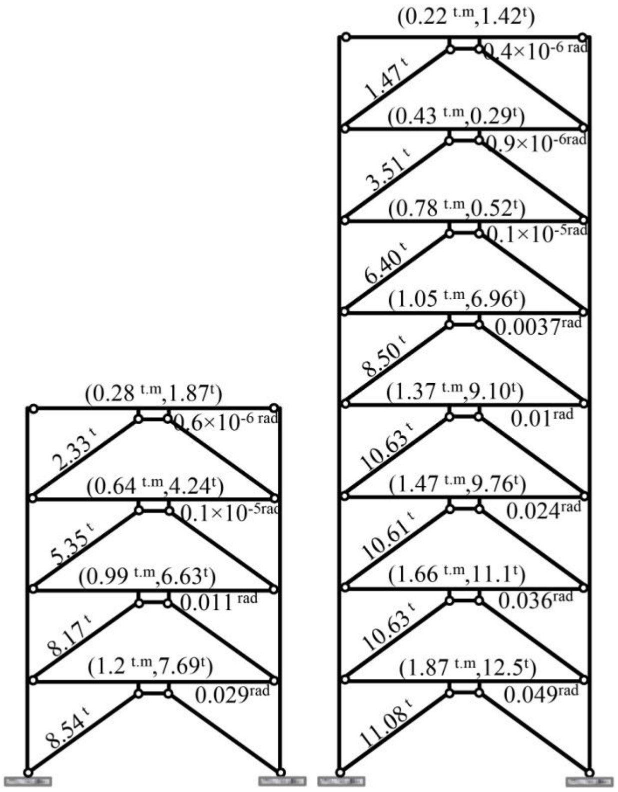

Fig. 9 Recorded parameters of the braced spans at the target displacement

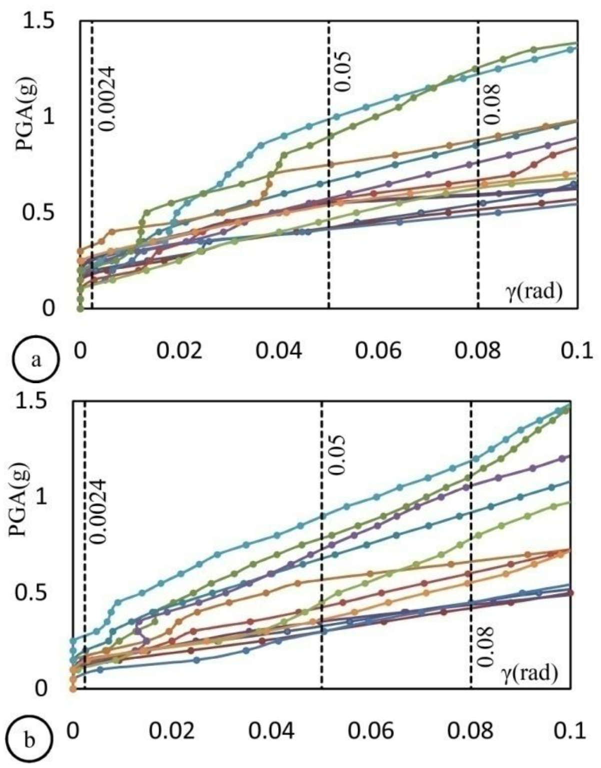

Fig. 10 Developed IDA curves and the limit states (a) 4-story (b) 8-story

performance of the system in dissipating seismic energy at the design hazard level according to the Iran's seismic design code (Standard No. 2800 2014). As it could be seen, axial strains of the braces are less than the tensile ones and compressive limit strains of the immediate occupancy performance level. So, all the braces in tension and compression perform in levels higher than the IO. It is the same for story beams at the braced spans. In this intensity level, yielding in shear or flexure is very unlikely. Control of the shear strain in the vertical links (Fig. 6) displays acceptable performance of the links in the design hazard level. Thus, the design objective is fulfilled.

3.3 Incremental dynamic analysis

This type of analysis consists of consecutive dynamic analysis, which aims to compute response of the structure for various intensities of ground motion excitations. In this method, the well-known concept of ground motion scaling is used and developed to a method by which it is possible to estimate demand and capacity of the structure for a wide range of elastic behavior to the point of collapse (Vamvatsikos and Cornell 2002). Nowadays, the incremental dynamic analysis (IDA) is one of the best methods for reliability evaluation and development of the fragility curves. It is possible to study effect of variation in different parameters of ground motions (domain, frequency content, duration and …) on the structural responses by means of this method. In the present study, IDA analysis is performed on the frames based on the probable ground motions. Selection of appropriate records and specifying damage and intensity measures are the prerequisites of IDA analysis.

3.3.1 Selection of accelerograms

The first step of IDA analysis is the selection of appropriate ground motion records. The selected accelerograms must reflect properties of the ground motions source, distance from the fault and its mechanisms, earthquake intensity and soil properties. In a statistical study, in addition to the properties of the records, number of them is also important. It is obvious that increasing number of ground motion records would reduce uncertainty of the earthquake parameters (inherent uncertainty). Studies revealed that selection of 10 or 20 earthquake records provides acceptable accuracy for the IDA analysis (Shome and Cornell 1999).

In the present section, 12 pair of ground motion records consistent with the soil type "II" (360(m/s)$\leq V_s \leq$760(*m/s*))) are selected from the PEER database (http://peer.berkeley.edu/peer-ground-motion-database).

The selected accelerograms are classified as far fault earthquakes. Among the horizontal components of the ground motions, the one which has higher spectral acceleration in the range of frequency vibration of the frame is selected as the main component for IDA analysis. Properties of these accelerograms are listed in Table 5.

3.3.2 Selection of the intensity parameters, seismic response and description of the results

Intensity of the applied accelerograms to the frame which increases step by step during analysis is characterized by *IM* and outcomes of the analysis in each step which is

Table 5 Average of the maximum ground acceleration to reach limit states of the vertical links (g)

Levels:	4 story frame	8 story frame
$\gamma = 0.0024(rad)$	0.21	0.151
$\gamma = 0.05(rad)$	0.57	0.45
$\gamma = 0.08(rad)$	0.75	0.65
$\gamma = 0.1(rad)$	0.85	0.75

Table 6 Share of each story from dissipation of total applied energy to the 4 story frame at different intensity levels (%)

Design Basis Earthquake (PGA=0.35 g)												
Story No.	R1	R2	R3	R4	R5	R6	R7	R8	R9	R10	R11	R12
1	74.19	88.8	71.46	90.1	67.12	100	76.55	77.54	81.51	57.96	90.82	85.36
2	22.58	9.67	13.65	7.92	10.55	0	12.16	17.36	14.14	23.67	9.18	5.83
3	3.23	1.53	14.89	1.98	22.33	0	11.29	5.1	4.35	18.37	0	8.81
4	0	0	0	0	0	0	0	0	0	0	0	0
Maximum Considered Earthquake (PGA=0.55 g)												
Story No.	R1	R2	R3	R4	R5	R6	R7	R8	R9	R10	R11	R12
1	69.23	74.4	72.46	71.46	65.26	83.75	65.01	74.7	71.84	49.66	71.46	69.7
2	23.77	20	11.66	23.6	17.12	14.4	25.3	19.35	21.22	21.84	21.72	20.87
3	7	5.6	15.88	4.94	17.62	1.85	9.69	5.95	6.94	28.5	6.82	9.43
4	0	0	0	0	0	0	0	0	0	0	0	0

Table 7 Share of each story from dissipation of total applied energy to the 8 story frame at different intensity levels (%)

Design Basis Earthquake (PGA=0.35 g)												
Story No.	R1	R2	R3	R4	R5	R6	R7	R8	R9	R10	R11	R12
1	45.41	45.78	58.56	48.4	42.4	64.14	42.3	49.5	42.18	82.38	45.9	36
2	27.3	26.9	22.8	26.8	15.14	27.8	23.2	25.56	23.82	7.69	25.68	16.63
3	13.9	14.4	2.6	12.41	4.34	6.26	12	8.44	10.3	0	12.66	7.32
4	4.34	4.6	0.26	3.23	1.89	0	4.22	1.49	2.23	0	4.47	4.22
5	6.95	5.33	6.82	6.33	21.96	1.8	10.42	9.67	10.42	0.75	4.34	18
6	1.49	1.74	1.86	1.86	6.83	0	4.96	3.97	6.7	0	4.22	14.23
7	0.61	1.25	7.1	0.97	7.44	0	2.9	1.37	4.35	9.18	2.73	3.6
8	0	0	0	0	0	0	0	0	0	0	0	0
Maximum Considered Earthquake (PGA=0.55 g)												
Story No.	R1	R2	R3	R4	R5	R6	R7	R8	R9	R10	R11	R12
1	34.49	36.85	44.79	36.97	37.1	50.5	37.97	40	37.34	50	40.45	37.97
2	22.95	24.57	21.1	23.82	16.25	28.16	23.95	25.19	22.95	16.38	26.18	20
3	16.5	16.25	8.31	15.26	8.93	12.53	13.9	14.64	14.6	1.12	15.38	12
4	10.67	9.56	1.33	10.53	5.71	3.27	8.06	6.37	6.83	0.61	6.33	7.32
5	9.55	7.94	8.2	8.3	11.66	3.47	7.81	7.2	8.56	7.82	6.9	12.28
6	4.6	3.47	7.07	3.72	9.18	1.36	5.33	4.1	5.83	12.16	2.6	6.83
7	1.24	1.36	9.2	1.4	11.17	0.71	2.98	2.5	3.89	11.91	2.16	3.6
8	0	0	0	0	0	0	0	0	0	0	0	0

the response is represented by *DM*. The IDA curve is graphical representation of the *IM* versus *DM*. It is needed to select appropriate *IM* and *DM* such that they represent earthquake effect and frame behavior in a well manner.

In the present study, the maximum ground acceleration *PGA*(*g*) is selected as intensity measure (*IM*) and the maximum shear deformation of the vertical links (γ) is opted as damage measure (*DM*). Fig. 10 represents the resulting curves and limit states for the vertical links in 4 and 8 story frame structures.

Then, the acceleration corresponding with different limit states of the vertical links are extracted from the IDA curves. Based on the average of the recorded value which is presented in Table 5, it is evident that the average of maximum acceleration necessary to reach high damage levels in the vertical links, is considerably higher than the maximum acceleration of the design earthquake (0.35 g). For the maximum probable earthquake (0.55 g) it is also expected that the shear strain in the vertical link to be less than 0.08 radian.

It is obvious that the required intensity for yielding of the vertical links is much lower than the intensity of the design earthquake, especially for the higher structures.

For the maximum acceleration equal to 0.35 g and 0.55 g (corresponding to the design basis and the maximum considered earthquakes, respectively), the percent of the applied energy dissipated by vertical links located at different stories are recorded and presented in Tables 6 and 7. As it could be seen, in each excitation, (R_i) is the sum of the story values which reaches to 100 percent. In this circumstance, it is obvious that the applied energy is completely absorbed and dissipated by the vertical links and the rest of the frame elements remain elastic. This observation once more proves that the vertical links are seismic fuse of the structure.

More than 50 percent of the applied energy to the frame is dissipated in links of the lower half of structure. It is obvious that the damage distribution along the length of the structure is controllable by increasing capacity of the story links.

For the stated intensity levels, the maximum drift and story shear under each ground motion are recorded and the average values are used for comparison as demonstrated in Figs. 11 and 12. As it could be seen in the Fig. 11, in both hazard levels, the maximum story drift is considerably less than the proposed admissible value by Iran's standard for the design hazard level (0.35 g).

This finding demonstrates reliability of this system for medium and high hazard levels in Iran. It is possible to provide uniform distribution of story drift f by changing capacity of the link sections. In this condition, the assumptions of first mode and triangular distribution of the lateral loads would be more acceptable.

According to Fig. 12, however, the trend of story shear variations for both exact time history and equivalent static analyses according to the 2800 code are similar, but their base shears are not equal. In the low rise structure, response of the time history analysis is about 24 percent more than the estimation of 2800 code, but for the higher structure, this difference is about 10 percent. This is more evident in the low rise structure and can be attributed to its considerable stiffness due to reasons such as selection of different types of structural members.

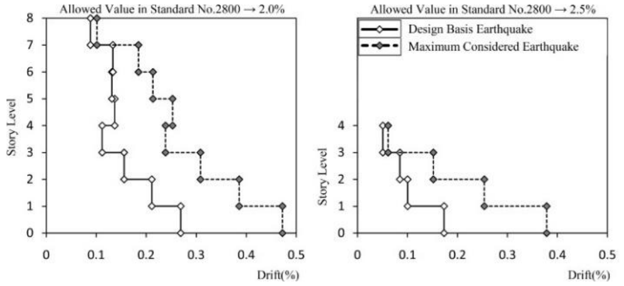

Fig. 11 Average of the maximum story drift in the design basis and maximum considered earthquakes

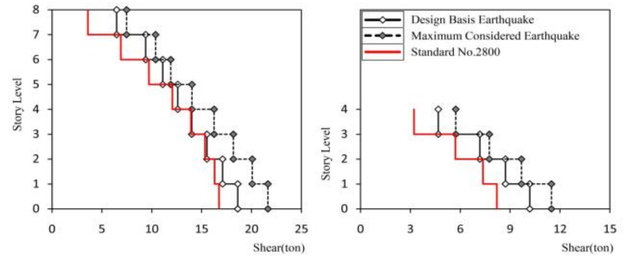

Fig. 12 Average of the maximum story shear under the design basis and the maximum considered earthquakes and the shear distribution according to Standard No. 2800

By increasing the hazard level to the maximum probable earthquake (1.5 times of the design earthquake intensity), increase of this parameter in 4 and 8 story frames is equal to 13 and 16 percent, respectively, which is less than 1.5 times of the design earthquake responses. This finding can be justified based on this fact that by increasing the intensity level, share of the vertical links in energy dissipation is also increased (Tables 6 and 7).

4. Fragility analysis

Due to various sources of uncertainty in the seismic performance of structures, it is obvious that exploiting probabilistic approaches for evaluation and judgment in this topic is more reasonable than deterministic methods (Ang and Tang 2007). In the reliability analysis, fragility curves are very important. Fragility function has the following mathematical form

$$Fragility = P\left[R > LS_i \mid IM = S\right] \quad (8)$$

In this relation, R is the structural response and LS_i is the corresponding limit state or performance level. IM is representative of the earthquake intensity and S is the presumed intensity. In fact, fragility curves present the cumulative probability density of damage (Beheshti-Aval *et al*. 2018). These curves are the result of statistical and probabilistic analyses and depending on the desired accuracy, various methods are available (Cimellaro *et al.* 2006). Currently, the fragility curves are constructed by analytical approach via IDA method. The aim of this section is to evaluate seismic reliability of the dual vertical link. For this purpose, two different scenarios are considered (Zareian *et al.* 2010).

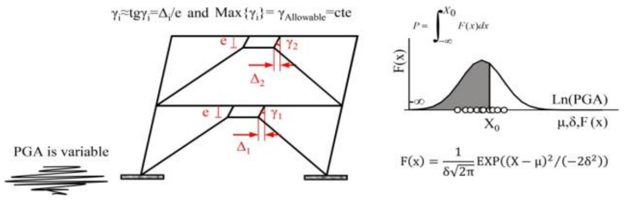

Fig. 13 Exceedance probability for deformations of the vertical links from the allowable limit state ($\gamma_{Allowable}$) at the given hazard level (X_0)

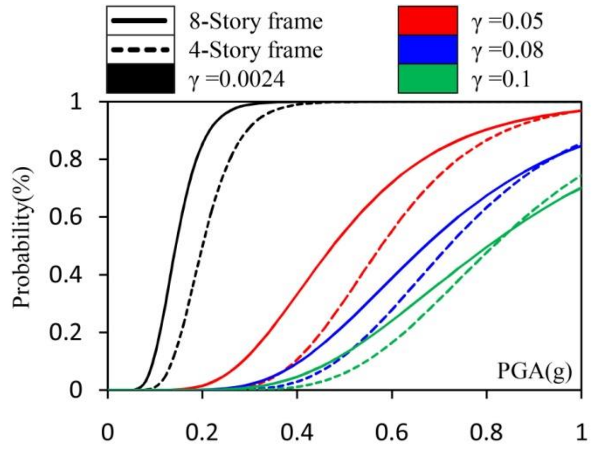

Fig. 14 Fragility curves for various limit states of the vertical links

Table 8 Exceedance probability of the shear strain in the vertical links from the limit states under the DBE (%)

Models	Limit States			
	0.0024	0.05	0.08	0.1
4 Story	96.85	4.44	1.01	0.34
8 Story	99.77	22.12	4.83	2.24

Table 9 Exceedance probability of the shear strain in the vertical links from the limit states under the MCE (%)

Models	Limit States			
	0.0024	0.05	0.08	0.1
4 Story	99.96	43.45	19.32	10.43
8 Story	99.99	64.2	30.64	18.01

4.4.1 Collapse based on the seismic intensity parameter (IM-based)

In this method, instead of specifying the intensity which results in a special performance level of the structure, the probability of reaching the given performance level for different earthquake intensities is computed. Because in this method, the selected seismic intensity parameter is determinant of the damage state of structure, fragility curves are developed for a given performance (damage) level. For the studied frames, the maximum shear deformation of the vertical links is selected as the response and the limit states defined in Fig. 6 for the strain are considered as damage criteria for frames. The quantitative values according to the mentioned figure (0.0024, 0.05,

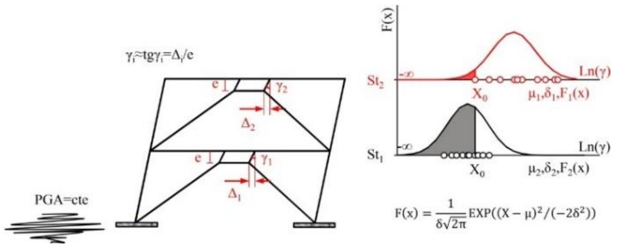
Fig. 15 Reliability of vertical links for a given performance level X_0 at a constant hazard level (PGA)

Table 10 Reliability of the vertical links in each story under the design basis earthquake (%)

4-Story	Limit States			
Story No.	0.0024	0.05	0.08	0.1
1	0.032	96.54	99.57	99.87
2	44.19	85.95	89.76	91.27
3	60.82	89.63	92.12	93.13
4	100	100	100	100
8-Story	Limit States			
Story No.	0.0024	0.05	0.08	0.1
1	0	71.67	90.54	95.19
2	0.05	90.48	97.84	99.1
3	31.2	72.13	77.44	79.74
4	59.5	84.6	87.3	88.43
5	25.2	91.97	95.76	96.97
6	32.26	94.73	97.4	98.2
7	45.67	87	90.64	92.1
8	100	100	100	100

Table 11 Reliability of the vertical links in each story under the maximum considered earthquake (%)

4-Story	Limit States			
Story No.	0.0024	0.05	0.08	0.1
1	0	54.1	83.56	91.8
2	0.032	85.2	95.87	98.05
3	1.2	98.47	99.78	99.92
4	100	100	100	100
8-Story	Limit States			
Story No.	0.0024	0.05	0.08	0.1
1	0	45.74	74.17	84.31
2	0.011	62.25	82.46	89
3	0.32	74.41	88.08	92.33
4	28.12	62.97	68.15	70.49
5	0	91.21	98.8	99.64
6	0	93.4	99.02	99.68
7	0	99.99	100	100
8	91.61	98.86	99.22	99.34

0.08 and 0.1) are assigned to these limit states. The process for developing fragility curves in this method is as follows:

In the first step, the maximum acceleration ($PGA(g)$) corresponding to the predefined values of shear strain in the vertical links $\gamma_{Allowable}$ are extracted from the curves during the IDA analysis (Fig. 10). In the next step, assuming the recorded values has the log-normal distribution, their probability density function (F(x)) is derived after computing mean value (μ) and the standard deviation (δ). According to Fig. 13, by replacing value of X_0 as the earthquake intensity, the area under the curve of the probability density function from $-\infty$ to X_0, is the probability of exceeding the related damage level. It means that for the given intensity, the probability that the responses of the vertical links reach the considered damage level is "P" (Mohsenian and Mortezaei 2018a). It is obvious that the difference between "P" and 1 indicates seismic reliability of the structure. The curve which is the result of repeating this process for various seismic intensity is called the "fragility curve" for the considered damage level. For the studied frame structures, the fragility curves are constructed according to the described approach and Fig. 14 demonstrates the result. Tables 8 and 9 present the quantitative values of exceeding the considered limit states for the design basis and the maximum considered earthquakes (DBE and MCE) which are extracted from the curves.

4.4.2 Collapse based on the seismic demand parameter (EDP-based)

In this approach, instead of specifying the intensity which causes a certain performance level in the structure, probability of reaching different limit states due to a given intensity level is determined. Therefore, the fragility curves are defined for constant earthquake intensity. The process is defined as follows:

All of the ground motion records are scaled to a constant hazard levels and then applied to the structures. Then, the maximum responses are extracted from the analysis results. Again, it is assumed that the recorded values have the log-normal distribution and after computation of the mean value (μ) and standard deviation (δ), a density distribution function (F(x)) is calculated for the recorded values.

According to Fig. 15, by replacing value of X_0 as the response corresponding to a desired damage level, the area under the curve of the probability density function from $-\infty$ to X_0, demonstrates the reliability of structure. In other words, for the given intensity, the probability that the responses of the vertical links do not reach the considered damage level, is "P". In this study, the reliability of the vertical links for each story is evaluated based on the explained approach and for the design (0.35 g) and the maximum probable (0.55 g) hazard levels. The results are presented in Tables 10 and 11.

This approach provides very useful information about damage distribution and energy absorption along the height of the structure. Based on the obtained results from both scenarios, it is concluded that under the evaluated levels, stress in the vertical links surely reaches yield level. However, the low rise structure always is more reliable, but under the design hazard level, for the higher damage levels of the links (higher than 0.05 radian), reliability of both frame structures is more than 70 percent. When this intensity level is considered by the designer, it is obvious that energy dissipation capacity of the studied system is available against the possible aftershocks.

As it could be deduced, the structural response is sensitive with respect to the applied excitation and the height of structure, and increase in these two parameters increases probability of occurrence of damage and performance levels.

5. Evaluation of response modification factor

Response modification factor is one of the most controversial topics in the seismic design standards. In many of investigations, researchers stated that the response modification factor suggested in the design codes (R_{Code}) is based on engineering judgments and are proposed based on experiences and performance observation of the existing structures under the past severe ground motions (Whittaker *et al.* 1999). It is obvious that a more accurate evaluation of this factor results in higher reliability of the code provisions (Bertro 1989). Unfortunately, it is not clear this factor is proposed for what hazard level and which performance level (possibly the life safety). Furthermore, it is not clear that to which hazard level, the suggested factors guaranty safety of the structure. In addition, reliability of the proposed response modification factors under the hazard level higher than the design earthquake of the codes is not known. However, there are many questions about these response modification factors. For example:

- Whether these factors are reliable for an arbitrary damage level?
- Is it logical to use a constant response modification factor for a system under various seismic hazards?

Based on the description of this section, it is possible to compute response modification factor for the structures according to the site seismic hazard or for a given damage level as the accepted performance level.

In this study, in addition to introduction and describing process for evaluation of demand response modification factor (R_{Demand}) and supply modification factor (R_{Supply}), a new method is proposed. According to the new proposition, in the new generation of design codes, the response modification factor for different systems could be proposed in multi-level form (for different hazard and performance levels) by matrix notation. This is in fact the main difference between the present study with the other similar papers about evaluation of the response modification factors.

In the following, concepts of three different types of response modification factors are described (Mohsenian and Mortezaei 2018a, b).

5.1 Design based response modification factor (R_{Code})

Because the ductility demand is not included in definition of R_{Code}, this method in the seismic design codes is also defined by the name of "force method". In Iran's seismic design code, the values for this factor are suggested only based on the structural system and material type and independent of vibration period. In this study, for the preliminary design of the frames equipped with dual links, the suggested value of 7 for the special eccentric frames is used (Standard No. 2800 2014).

5.2 Demand (displacement/ductility) response modification factor (R_{Demand})

This type of response modification factor is computed based on the site seismic hazard. Moreover, the physical and geometrical properties of the structure affect this factor. The results of researches revealed that intensity and focal depth of earthquake has no effect on R_{Demand}, but parameters such as ductility, energy absorption capacity, height and vibration period of structure, over-strength, indeterminacy, number of degrees of freedom and soil type, are influential (Lia and Biggs 1980, Miranda 1991, ATC19 1995a). In this study, the demand response modification factor is computed by the following relation, in which R_{μ}^{SDOF} is the Response Modification Factor (RMF) due to ductility and dissipated energy by hysteresis behavior of equivalent single degree of freedom system

$$R = R_{\mu}^{SDOF}.R_m.\Omega_S.R_d \tag{9}$$

R_m is the response modification factor for the number of degrees of freedom (Moghaddam and Karami Mohammadi 2001, Santa-Ana 2004). Because in this study, the response modification factor is computed directly for the multi degree of freedom system, effect of the degrees of freedom is directly included in the ductility factor ($R_{\mu}^{MDOF} = R_{\mu}^{SDOF}.R_m$). Therefore, it is possible to rewrite the Eq. (9) in a more simple form

$$R = R_{\mu}^{MDOF}.\Omega_S.R_d \tag{10}$$

Ω_s is the over-strength factor that incorporates the effects of indeterminacy of structure implicitly and R_d is the allowable stress factor. While in the allowable stress design and the limit state method design, the loads and strength of materials are multiplied by factors, this is necessary to reduce forces using this allowable stress factor. The mentioned factors are derived using the following relations (Fanaie and AfsarDizaj 2014)

$$R_{\mu}^{MDOF} = V_e/V_y \tag{11}$$

$$\Omega_S = V_y/V_S \tag{12}$$

$$R_d = V_S/V_d \tag{13}$$

The parameters used in these relations are as follows:

V_e is the elastic base shear. The scaled accelerograms of a certain hazard level (demand earthquakes) are applied to the structure with the assumption of elastic behavior and average of the recorded base shear value is taken as the elastic base shear. Because in this study, the design earthquake based on Iran' seismic design code is considered, to achieve more compatibility with the site condition, the artificial accelerograms produced in section (4-2) are used.

V_y is the yield base shear. Demand earthquakes are applied to a nonlinear structure and average of the maximum roof drift is computed. The value of V_y is derived from the idealized Push-over capacity curve according to the ASCE41-13 (2014), by using this mean value, which is the maximum drift corresponding with design basis earthquake (Table 3), as the target displacement.

The base shear corresponding to initiation of nonlinear behavior in the structure is characterized by V_s. According to Fig. 16, this quantity is the separation point between the linear and nonlinear capacity curves of the structure.

The design base shear, V_d, is also computed by dividing the results of multiplication of computed spectral acceleration from the linear spectrum of structure and total weight of structure by the code response modification factor, i.e., $(Sa.W/R_{Code})$. Finally, the demand response modification factor of structure is computed by replacing values derived from Eqs. (11) to (13) in Eq. (10). In Tables 12 and 13, the necessary parameters for computation of the demand response modification factors are listed.

5.3 Available strength response modification factor (R_{supply})

The supply response modification factor is determined based on the capacity of structure in sustaining nonlinear deformation and allowable damage levels. Design of structures could be performed based on the force method or selection of the strength reduction factor by assuming a specific damage level under the design earthquake. This is the performance idea that is used for seismic performance evaluation of the structures nowadays (Fajfar 2000). Computation of the response modification factor for the frames based on the lateral strength and according to the American approach (ATC-40 1996, Mwafy and Elnashai 2002) is as follows:

IDA analysis is performed on the structure in the nonlinear range of behavior by using ground motion records that are compatible with site condition and the considered damage PGA coefficients (in this study, drifts corresponding to maximum strength and initiation of yielding in the story beams and reaching shear strains equal to 0.05, 0.08 and 0.1 radian in the vertical links) are recorded. In the following, linear dynamic analysis is performed on the structure using the recorded PGAs of the previous step and the base shear (V_e) is evaluated. In the next step, push-over analysis is performed by taking advantage of the modal lateral load pattern and the capacity curve of structure is constructed. The derived curve is idealized as a bilinear curve according to ASCE41-13 (2014) and finally, the yield base shear (V_y) is calculated. The next steps are same as those used for calculation of the demand response modification factor (Eqs. (11) to (13)). The necessary parameters for computing the supply response modification factors for the studied frame structures are listed in Tables 12 and 13. It is noteworthy to say that in these tables, the parameters R^1_{Supply}, R^2_{Supply} and R^3_{Supply} are the factors corresponding to the occurrence of shear strains equal to 0.05, 0.08 and 0.1, respectively, in the vertical links and R^4_{Supply} is corresponding with the yielding and damage of the story beam.

As it could be seen, the supply response modification factor of the studied frame structures and the corresponding hazard level, are evaluated higher than the demand response

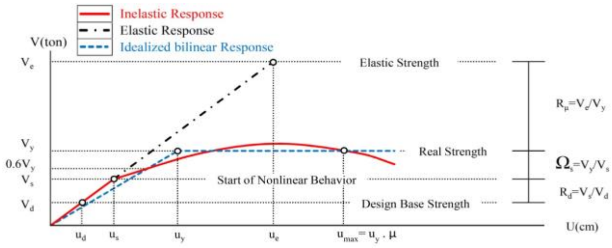

Fig. 16 Idealization of capacity curve and the parameters used for determining response modification factor

Table 12 Response reduction factors of code, demand and capacity for the 4-story frame

Shear values are reported in (Ton)	R-Factors					
	R_{code}	R_{Demand}	R^1_{Supply}	R^2_{Supply}	R^3_{Supply}	R^4_{Supply}
Average of the PGA(g)	0.35	0.35	0.56	0.74	0.85	1.06
Elastic strength (V_e)	*	25.83	34.6	45.77	52.06	71.4
Real strength (V_y)	*	11.32	11.52	11.79	11.83	12.01
strength for the start of nonlinear behaviors (V_s)	*	10.9	10.9	10.9	10.9	10.9
Design base strength (V_d)	*	8.2	8.2	8.2	8.2	8.2
RMF due to ductility (R_μ)	*	2.28	3.00	3.88	4.40	5.94
RMF due to over strength (Ω_s)	*	1.04	1.05	1.08	1.08	1.1
RMF due to allowable stress (R_d)	*	1.33	1.33	1.33	1.33	1.33
RMF ($R = R_\mu.\Omega_S.R_d$)	7.00	3.15	4.22	5.58	6.35	8.7

Table 13 Response reduction factors of code, demand and capacity for the 8-story frame

Shear values are reported in (Ton)	R-Factors					
	R_{code}	R_{Demand}	R^1_{Supply}	R^2_{Supply}	R^3_{Supply}	R^4_{Supply}
Average of the PGA (g)	0.35	0.35	0.45	0.64	0.73	0.896
Elastic strength (V_e)	*	43.53	52	67.06	80.00	114.1
Real strength (V_y)	*	15.47	15.58	15.69	16.15	16.57
strength for the start of nonlinear behaviors (V_s)	*	14.04	14.04	14.04	14.04	14.04
Design base strength (V_d)	*	16.74	16.74	16.74	16.74	16.74
RMF due to ductility (R_μ)	*	2.81	3.34	4.27	4.95	6.88
RMF due to over strength (Ω_s)	*	1.1	1.11	1.12	1.15	1.18
RMF due to allowable stress (R_d)	*	1	1	1	1	1
RMF ($R=R_\mu.\Omega_s.R_d$)	7.00	3.10	3.70	4.77	5.7	8.12

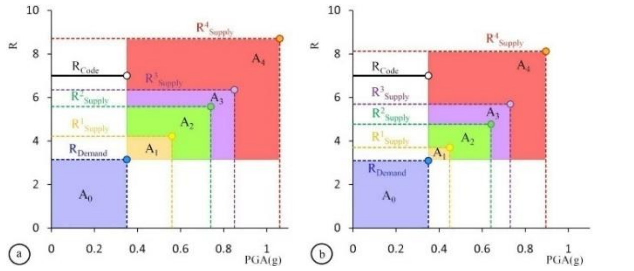

Fig. 17 Comparison of demand, supply and code response modification factors in (a)_4story frame (b) -8story frame

Table 14 Matrix of the response modification factors for the 4-story frame

Hazard Levels	Limit States:			
	γ=0.05rad	γ=0.08rad	γ=0.1rad	Beam damage
PGA_A=0.35 g	4.22	*	*	*
PGA_B=0.55 g	4.22	*	*	*
PGA_C=0.65 g	*	5.58	*	*
PGA_D=0.75 g	*	*	6.35	*

Table 15 Matrix of the response modification factors for the 8-story frame

Hazard Levels	Limit States:			
	γ=0.05rad	γ=0.08rad	γ=0.1rad	Beam damage
PGA_A=0.35 g	3.7	*	*	*
PGA_B=0.55 g	*	4.77	*	*
PGA_C=0.65 g	*	*	5.7	*
PGA_D=0.75 g	*	*	*	8.12

modification factor and the design hazard level, correspondingly. This denotes high strength and sufficient safety of the eccentric braced frames equipped with the dual vertical links under the high hazard levels in Iran (Fig. 17).

In the frames, for each pair value in the A_0 range, the system surely would not experience any of the limit states. Therefore, if in the response modification equal to 3 is used by the designer for the design earthquake (or the lower hazard levels) according to the 2800 code, the strain in the link beam would be negligible.

It is obvious that opting the response modification factor in the range between the damned and supply values corresponding to a specific performance level of the frame guaranties that the system remains in this performance level or lower levels. For example, for each pair in the yellow area of the figure (A_1), strains in the link beam are less than 0.05 radian, or for each pair value in the purple area (A_3), strains of the link beam are less than 0.08 radian.

Therefore, selection of the code response modification factor equal to 7 for the preliminary analysis will guaranty safety of the frame and energy absorption of the lateral load bearing elements under the design earthquake, without any yielding in the story beams and the code response modification factor is always in the safe threshold.

Based on Fig. 17, for the design earthquake and lower intensities, the maximum response modification factor which is safe, would be 8.

Noteworthy, to derive a general conclusion towards the response modification factor of the system studied herein, further analyses on the analytical models including the factors effective on the structural responses, are highly required. However, this study can make the ground for the future studies.

Parametric studies show that increase in the height of structure results in increase in the ductility (R_μ) and over-strength factors (Ω_s) for demand and supply response modification factors. In each frame, the mentioned factors (R_μ, Ω_s) increase by rising the damage level. This is more evident for the ductility factor.

According to the abovementioned, it is possible to propose response modification factor for each intensity level and performance level in a matrix form (Tables 14 and 15).

It should be noted that in these matrices, the selected hazard levels are completely arbitrary. In the hazard level B, for the 4 story frame structures, strain of the vertical link is less than 0.05 radian. Assuming this hazard level is considered by designer, the frame would not experience higher performance levels. Therefore, for this intensity level no value for the other damage levels is presented in the matrix. When the response modification factor is taken equal to 4.22 (and lower), in the hazard level “B” and lower intensities, no vertical link experiences shear strain equal to 0.05 radian. In this hazard level, when the response modification factor for the 8 story frame is 4.77 (or lower), surely the shear strain in the vertical link would be less than 0.08 radian.

It is apparent when this idea is included in the new generation of design codes for different structural systems and by considering at least three hazard level (service, design and maximum probable earthquakes) and three performance levels (immediate occupancy, life safety and collapse prevention), a great improvement in the financial and safety aspects of the design process will occur.

6. Conclusions

The obtained conclusions which are limited to the utilized models and assumption of this study, are as follows:

• For the eccentric braced frame structures equipped with dual vertical links, due to period of the first vibration mode (less than 1 second) and coefficient of effective translational mass (more than 75 percent), the assumption of triangular lateral load pattern and the use of equivalent static method for analysis and design of structure are acceptable.

• The available empirical relations in the design codes for evaluation of the vibration period unconventional structural systems such as moment frames or special eccentric or concentric braced frames provide poor estimations for the new system. Due to high stiffness of the system, utilizing empirical relation of the highly ductile systems leads to considerable errors in estimation of the vibration period and the earthquake forces in the structure.

• Under the design and the maximum probable earthquakes, average of the maximum story drifts of the system is by far less than the allowable code drifts. Accordingly, this system is applicable for improving lateral stiffness of damaged structural systems.

• Distribution of shear forces along the height of structure based on the equivalent static method and the nonlinear dynamic analysis are in good agreement. Nevertheless, the base shear of 4 and 8 story structures based on the equivalent static methods in comparison with the dynamic responses are 24 and 10 percent higher, respectively.

• The vertical links are the first elements which experience damage under the seismic loading. They absorb and dissipate all of the applied energy to the frame. Therefore, the assumption of seismic fuse role for the vertical links and elastic behavior of the other structural members is correct.

• Stress and strain variation rate in the vertical links of each story is the same. In each story, by yielding of the links, the force level of braces remains constant. Thus, design of the braces and determination of the lateral stiffness of structure only depends on the capacity and geometric properties of the fuses.

• Design of the new system is very flexible and using the vertical links increase seismic reliability of the structure. Designers could easily control damage distribution in the height of the structure and story drifts by changing the fuse sections.

• Under the design hazard level (0.35 g), shear yielding surely occurs in the vertical link of the 4 and 8 story buildings. Under the maximum probable earthquake (0.55 g), the probability that the shear strain of the links exceed the allowable limit state of codes (0.08 radian) is less than 32 percent for the studied structures. This proves high seismic reliability of the system under severe ground motions and acceptable energy absorption under medium intensity ground motions.

• According to the site seismic hazard level, the response modification factor (R_{Demand}) for the frame is computed about 3. The response modification factor for the ultimate strength (collapse of the beams) and the corresponding intensity for the 4 story frame are 8.7 and 1.06 g, respectively. These values for the 8 story frame structure are equal to 8.12 and 0.896 g (R^4_{Supply}). It is obvious that the corresponding intensities are remarkably higher than the design (0.35 g) and the maximum considered (0.55 g) earthquakes.

• By increasing height of the structures and the performance level, the ductility and over-strength factors (R_μ, Ω_s) for both demand and supply response modification factors increase. This is more evident in the case of ductility factor.

Finally, based on the mentioned capabilities and advantages, it is concluded that the eccentric braced frame system equipped with dual vertical links, in addition to its application in seismic rehabilitation and strengthening the damaged structures, is applicable as a main lateral load bearing system (by itself or in combination with other systems) for design of structures and could be included in the future seismic design codes.

References

ABAQUS (2014), *Version 6.14, ABAQUS User's Manual, SIMULIA World Headquarters*, U.S.A.

Ang, A.H.S. and Tang, W.H. (2007), *Probability Concepts in Engineering: Emphasis on Applications to Civil and Environmental Engineering*, 2nd Edition, Wiley, University of Michigan, U.S.A.

ASCE/SEI Standard 41-13 (2014), *Seismic Evaluation and Retrofit of Existing Buildings*, American Society of Civil Engineers, Reston, Virginia, U.S.A.

ATC (1995a), *Structural Response Modification Factors*, ATC-19 Report, *Applied Technology Council*, Redwood City, California, U.S.A.

ATC (1996), *Seismic Evaluation of Concrete Buildings*, Vol. 1, ATC-40, Applied Technology Council, Redwood, California, U.S.A.

Baradaran, M.R., Hamzezarghani, F., RastegariGhiri, M. and Mirsanjari, Z. (2015), "The effect of vertical shear-link in improving the seismic performance of structures with eccentrically bracing systems", *Int. J. Civil Environ. Eng.*, **9**(8), 1078-1082.

Bathaei, A. and Zahrai, S.M. (2017), "Investigation of the effects of vertical link beam length on steel structures residual displacement", *Modar. Civil Eng. J.*, **17**(3), 47-60.

Beheshti-Aval, S.B., Mohsenian, V. and SadeghKouhestani, H. (2018), "Seismic performance-based assessment of tunnel form buildings subjected to near- and far-fault ground motions", *Asian J. Civil Eng.*, **19**(1), 79-92.

Bertro, V.V. (1989), "Evaluation of response reduction factors recommended by ATC and SEAOC", *Proceedings of the 3rd U.S. National Conference on Earthquake Engineering*, South Carolina, U.S.A.

Bouwkamp, J., Vetr, M.G. and Ghamari, A. (2016), "An analytical model for inelastic cyclic response of eccentrically braced frame with vertical shear link (V-EBF)", *Case Stud. Struct. Eng.*, **6**, 31-44.

Cimellaro, G.P., Reinhorn, A.M., Bruneau, M. and Rutenberg, A. (2006), *Multi-Dimensional Fragility of Structures: Formulation and Evaluation*, Multidisciplinary Center for Earthquake Engineering Research, MCEER-06-0002.

Computers and Structures, Inc. (CSI) (2015), *Structural and Earthquake Engineering Software*, ETABS, Extended Three Dimensional Analysis of Building Systems Nonlinear, Version 15.2.2, Berkeley, California, U.S.A.

Computers and Structures, Inc. (CSI) (2016), *Structural and Earthquake Engineering Software*, PERFORM-3D Nonlinear Analysis and Performance Assessment for 3-D Structures, Version 6.0.0, Berkeley, California, U.S.A.

Duan, L. and Su, M. (2017), "Seismic testing of high-strength steel eccentrically braced frames with a vertical link", *Proceedings of the Institution of Civil Engineers-Structures and Buildings*, **170**(11), 874-882.

Fajfar, P. (2000), "A nonlinear analysis method for performance based seismic design", *Earthq. Spectr.*, **116**(3), 573-592.

Fanaie, N. and AfsarDizaj, E. (2014) "Response modification factor of the frames braced with reduced yielding segment BRB", *Struct. Eng. Mech.*, **50**(1), 1-17.

Hancock, J., Watson-Lampre, J., Abrahamson, N.A., Bommer, J.J., Markatis, A., McCoy, E. and Mendis, R. (2006) "An improved method of matching response spectra of recorded earthquake ground motion using wavelets", *J. Earthq. Eng.*, **10**(spec01), 67-89.

Institute of National Building Regulations (2008), *Design and Construction of Steel Structures*, Topic 10, Ministry of Roads & Urban Development, Iran.

Lia, S.P. and Biggs, J.M. (1980), "Inelastic response spectra for

seismic building design", *J. Struct. Div.*, **106**(ST6), 1295-1310.
Lian, M. and Su, M. (2017), "Seismic performance of high-strength steel fabricated eccentrically braced frame with vertical shear link", *J. Constr. Steel Res.*, **137**, 262-285.
Massah, S.R. and Dorvar, H. (2014), "Design and analysis of eccentrically braced steel frames with vertical links using shape memory alloys", *Smart Mater. Struct.*, **23**(11), 115015.
Miranda, E. (1991), "Seismic evaluation & upgrading of existing buildings", Ph.D. Dissertation, University of California, Berkeley, U.S.A.
Moghaddam, H. and KaramiMohammadi, R. (2001), "Ductility reduction factor of MDOF shear-building structures", *J. Struct. Eng.*, **5**(3), 425-440.
Mohsenian, V. and Mortezaei, A. (2018a), "Evaluation of seismic reliability and multi level response reduction factor (R factor) for eccentric braced frames with vertical links", *Earthq. Struct.*, **14**(6), 537-549.
Mohsenian, V. and Mortezaei, A. (2018b), "A new energy-absorbing system for seismic retrofitting of frame structures with slender braces", *Bullet. Earthq. Eng.*, Accepted.
Mwafy, A.M. and Elnashai, A.S. (2002), "Calibration of force reduction factors of RC buildings", *J. Earthq. Eng.*, **6**(2), 239-273.
PEER Ground Motion Database, Pacific Earthquake Engineering Research Center.
Permanent Committee for Revising the Standard 2800 (2014), *Iranian Code of Practice for Seismic Resistant Design of Buildings*, 4th Edition, Building and Housing Research Center, Tehran, Iran.
Rahnavard, R., Hassanipour, A., Suleiman, M. and Mokhtati, A. (2017), "Evaluation on eccentrically braced frame with single and double shear panels", *J. Build. Eng.*, **10**, 13-25.
Daryan, S.A., Bahrampoor, H., Ziaei, M., Golafshar, A. and Assareh, M.A. (2008), "Seismic behavior of vertical shear links made of easy-going steel", *Am. J. Eng. Appl. Sci.*, **1**(4), 368-377.
Sabouri-Ghomi, S. and Saadati, B. (2014), "Numerical modeling of links behavior in eccentric bracings with dual vertical links", *Numer. Meth. Civil Eng.*, **1**(1), 14-20.
Santa-Ana, P.A. (2004), "Estimation of strength reduction factors for elastoplastic structures: Modification factors", *Proceedings of the 13th World Conference on Earthquake Engineering*, Vancouver, Canada, May.
Seki, M., Katsumata, H., Uchida, H. and Takeda, T. (1988), "Study on earthquake response of two-storied steel frame with Y-shaped braces", *Proceedings 9th World Conference on Earthquake Engineering*, Tokyo-Kyoto, Japan.
Shayanfar, M., Rezaeian, A. and Taherkhani, S. (2008), "Assessment of the seismic behavior of eccentrically braced frame with double vertical link (DV-EBF)", *Proceedings of the 14th World Conference on Earthquake Engineering*, Beijing, China, October.
Shayanfar, M.A., Barkhordari, M.A. and Rezaeian, A.R. (2011), "Experimental study of cyclic behavior of composite vertical link in eccentrically braced frames", *Steel Compos. Struct.*, **12**(1), 13-29.
Shome, N. and Cornell, C.A. (1999), *Probabilistic Seismic Demand Analysis of Nonlinear Structures*, Reliability of Marine Structures Report No: RMS-35, Civil and Environmental Engineering, Stanford University, U.S.A.
Vamvatsikos, D. and Cornell, C.A. (2002), "Incremental dynamic analysis", *Earthq. Eng. Struct. Dyn.*, **31**(3), 491-514.
Vetr, M.G., Ghamari, A. and Bouwkamp, J. (2017), "Investigating the nonlinear behavior of eccentrically braced frame with vertical shear links (V-EBF)", *J. Build. Eng.*, **10**, 47-59.
Whittaker, A., Hart, G. and Rojahn, C. (1999) "Seismic response modification factors", *J. Struct. Eng.*, **125**(4), 438-444.
Zahrai, S.M. and Mahroozadeh, Y. (2010), "Experimental study of using vertical link beam to improve seismic performance of steel buildings", *J. Civil Survey. Eng.*, **44**(3), 379-393.
Zahrai, S.M. and MoslehiTabar, A. (2013), "Analytical study on cyclic behavior of chevron braced frames with shear panel system considering post-yield deformation", *Can. J. Civil Eng.*, **40**(7), 633-643.
Zahrai, S.M. and Parsa, A. (2015), "Effect of flange width of vertical link beam on cyclic behavior of chevron braced Steel frames", *J. Seismol. Earthq. Eng.*, **17**(4), 281-292.
Zareian, F., Krawinkler, H., Ibarra, L. and Lignos, D. (2010), "Basic concepts and performance measures in prediction of collapse of buildings under earthquake ground motions", *Struct. Des. Tall Spec. Build.*, **19**(1-2), 167-181.

CC